Heliyon 10 (2024) e37275

Contents lists available at ScienceDirect

Heliyon

journal homepage: www.cell.com/heliyon

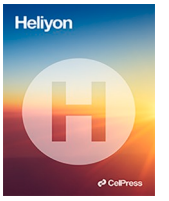

Research article

Effect of allyl isothiocyanate on 4-HNE induced glucocorticoid resistance in COPD and the underlying mechanism

WenLi Chang [a,1], MengWen Wang [a,1], WenTao Zhu [a], TingTing Dai [a], ZhiLi Han [a], NianXia Sun [a], DianLei Wang [a,b,c,*]

[a] School of Pharmacy, Anhui University of Chinese Medicine, Hefei, Anhui, 230012, China
[b] Anhui Province Key Laboratory of Research & Development of Chinese Medicine, Hefei, Anhui, 230012, China
[c] Anhui Province Key Laboratory of Pharmaceutical Preparation Technology and Application, Hefei, Anhui, 230012, China

ARTICLE INFO

Keywords:
4-Hydroxy-2-nonenal
Allyl isothiocyanate
COPD
Glucocorticoid resistance
Histone deacetylase 2

ABSTRACT

Chronic obstructive pulmonary disease (COPD) is a progressive inflammatory condition, and its clinical management primarily targets bronchodilation and anti-inflammatory therapy. However, these treatments often fail to directly address the progression of COPD, particularly its associated glucocorticoid (GC) resistance. This study elucidates the mechanisms underlying GC resistance in COPD and explores the therapeutic potential of allyl isothiocyanate (AITC) in modulating MRP1 transport. We assessed the levels of the oxidative stress product 4-HNE, HDAC2 protein, inflammatory markers, and pulmonary function indices using animal and cell models of GC-resistant COPD. The cascade effects of these factors were investigated through interventions involving AITC, protein inhibitors, and dexamethasone (DEX). Cigarette smoke-induced oxidative stress in COPD leads to the accumulation of the lipid peroxidation product 4-HNE, which impairs HDAC2 protein activity and diminishes GC-mediated anti-inflammatory sensitivity due to disrupted histone deacetylation. AITC regulates MRP1, facilitating the effective efflux of 4-HNE from cells, thereby reducing HDAC2 protein degradation and restoring dexamethasone sensitivity in COPD. These findings elucidate the mechanism of smoking-induced GC resistance in COPD and highlight MRP1 as a potential therapeutic target, as well as the enormous potential of AITC for combined GC therapy in COPD, promoting their clinical applications.

1. Introduction

Cigarette smoking-induced COPD not only diminishes the therapy efficacy but also leads to the exacerbation of inflammation and increased mortality [1]. Although bronchodilation intervention and broad-spectrum anti-inflammatory agents have exhibited significant effectiveness, the emergence of GC resistance has meant that the pulmonary function of COPD fails to achieve the goals recommended by the Global Initiative for Chronic Obstructive Lung Disease (GOLD) guidelines, creating substantial challenges for society and hospital management of COPD. Indeed, GC resistance has been implicated in cellular oxidative stress (OS) and histone acetylation, resulting in signaling pathway inhibitors and antioxidants have attracted considerable attention recently [2–4]. However, OS has not yet evolved into a therapeutic pathway for GC resistance of COPD clinically, primarily due to the lack of validation in the

* Corresponding author. School of Pharmacy, Anhui University of Chinese Medicine, Hefei, Anhui, 230012, China.
E-mail address: dlwang@ahtcm.edu.cn (D. Wang).
[1] These authors contributed equally to this work.

https://doi.org/10.1016/j.heliyon.2024.e37275
Received 20 February 2024; Received in revised form 29 August 2024; Accepted 30 August 2024
Available online 3 September 2024

pertinent pathophysiological mechanisms [5]. Therefore, it's necessary to uncover the interactions between GC resistance and oxidative stress in COPD, and propose effective regulatory strategies.

According to the several identified molecular mechanisms of GC resistance, apart from maintaining GRα expression and blocking signals with phosphodiesterase 4 inhibitors like roflumast and p38 MAP kinase inhibitors, reducing histone deacetylase 2 (HDAC2) expression has shown significant improvement [6,7]. Pro-inflammatory transcription factors, such as nuclear factor kappa-B (NF-κB) and activator protein 1 (AP-1), bind to intrinsic histone acetyltransferase in chronic inflammation, resulting in the acetylation of core histones around chromosomal DNA and subsequently activating the coordinated expression of various inflammatory genes [8]. GCs reverse this process by recruiting histone deacetylase-2 (HDAC2) to deacetylate the highly acetylated histones, thereby exerting their anti-inflammatory effects [9]. Notably, cigarette smoke could induce post-translational modifications, including nitrosylation, phosphorylation, and ubiquitination, which subsequently trigger the degradation of HDAC2 in a lung macrophage-dependent manner. This leads to a substantial decrease in the activity and expression of HDAC2 within alveolar macrophages, ultimately resulting in the development of GC resistance features in COPD patients [10–12]. Furthermore, the reactive oxygen species (ROS) and oxidants from cigarette smoke, coupled with inflammatory responses and antioxidant imbalance, predispose COPD to oxidative stress, thereby elevating the levels of lipid peroxidation products through the direct or indirect oxidation of amino acids, such as 4-hydroxynonenal (4-HNE) and malondialdehyde (MDA), which exhibit a negative correlation with pulmonary function [13,14]. Moreover, such reactive molecules deplete the thiol pool or react with proteins through carbonylation to form aldehyde-lipid adducts, ultimately disrupting the functionality and stability of intracellular (such as HDAC, nuclear factor erythroid 2-related factor 2, or Keap1) and extracellular matrix (ECM) proteins. Such a process can induce various cellular and biochemical effects, including the initiation and exacerbation of pulmonary inflammatory damage [15]. Therefore, these issues force us to investigate the relationship between HDAC2 expression and GC resistance in COPD, thereby tailoring treatment strategies and improving outcomes.

Multidrug resistance-associated protein-1 (MRP1), an ATP-dependent transmembrane efflux transporter located on the basolateral side of bronchial epithelial cells in the lungs, can effectively expel inhaled chemical foreign substances or toxins [16]. Therefore, the MRP1-mediated transport of cigarette smoke particulates or lipid peroxidation products represents an effective strategy for regulating oxidative stress damage [17]. Indeed, research has revealed that allyl isothiocyanate (AITC), derived from Chinese medicine Semen Sinapis Albae, not only upregulated the expression of MRP1 through Nrf2 and Notch1, but also inhibited the AhR/CYP1A1 pathway and activated the Nrf2/NQO1 pathway, thereby improving lung oxidative stress and delaying the pathological progression of COPD [18,19]. Consequently, we hypothesis that the increased MRP1 activity induced by AITC can facilitate the efflux transport of oxidative stress products, reducing HDAC2 damage and mitigating GC resistance pathways in COPD treatment. This study aimed to investigate the cascade effects of AITC, MRP1, oxidative stress, HDAC2, and GC resistance, thereby providing novel insights into the mechanisms of GC resistance in COPD and offering new avenues and clinical strategies for treatments.

2. Materials and methods

2.1. COPD models and groups

Male SD rats (180–220 g, n = 60) were procured from the Experimental Animal Center of Anhui Medical University (Anhui, China). The rats were acclimatized with adaptive feed for one week under conditions of relative humidity (55 ± 10 %) and temperature (25 ± 2 °C). They were randomly divided into two groups: the normal group (n = 10) and the COPD model group (n = 50). The COPD model was induced through a combination of exposure to cigarette smoke (Anhui China Tobacco Industrial Company, nicotine 0.8 mg, tar 10 mg) and the infusion of lipopolysaccharide (LPS) (Biosharp Company). Rats in the model group were exposed to smoke in a homemade fumigation box for 1 h, twice daily, for 60 days. The rats in the model group were anesthetized with 20 % urethane (1 g/kg) to expose the trachea, followed by the administration of 0.2 mL (1 mg/mL) lipopolysaccharide solution. The care and use of animals followed the guidance of Anhui University of Chinese Medicine Laboratory Animal Ethics and Management Committee (AHUCM-rats-2021,020).

Following successful modeling, the rats were randomly divided into four groups (n = 10), and treatment lasted for 15 days: the COPD group, the AITC group (80 mg/kg/day), the dexamethasone (DEX) group (27 mg/kg/day), and the combined AITC (80 mg/kg/day) and dexamethasone (27 mg/kg/day) group [20]. Equal amounts of corn oil were administered by gavage to the control and COPD groups.

2.2. Determination of lung function and processing of tissues

Rats in all groups were anesthetized with 20 % urethane (1 g/kg). Following this, tracheotomy and tracheal intubation were performed, and pulmonary function was assessed using a pulmonary function tester (AniRes2005, Beijing Berambo Technology Company). Parameters automatically recorded by the software included maximum flow in the middle of expiration (MMF), the ratio of 0.3-s forced expiratory volume to percent forced vital capacity (FEV0.3/FVC%), forced mid-expiratory flow (FEF25-75), and peak expiratory flow (PEF). At the end of the pulmonary function test, serum was prepared, and the right main bronchus was ligated. The left lung was then lavaged three times with sterile PBS (3 mL) via tracheal intubation, and the lavage fluid was collected. The right lung was rapidly fixed with 4 % paraformaldehyde, and the left lung was stored at −80 °C for subsequent experiments. Cells were counted using a hemocytometer. Cells were precipitated by centrifugation at 1200 rpm for 10 min at 4 °C, then stained on slides with Wright-Giemsa stain to calculate the proportions of eosinophils and neutrophils based on morphological criteria.

2.3. Lung tissue pathology and immunohistochemistry

The paraffin-fixed lung tissues were cut into 4 μm thick sections and stained with Hematoxylin-eosin (H&E). Then, the pathological damage to lung tissues was quantified by measuring the mean linear intercept using ImageJ software. Immunohistochemistry was employed to detect the expression of HDAC2 and 4-HNE in lung tissue. After dewaxing and hydrating, the lung sections were incubated in bovine serum (Beijing Zhongshan Golden Bridge Company) for 30 min. Subsequently, the lung tissue sections were incubated overnight at 4 °C with anti-HDAC2 antibody (1:1000) and anti-4-HNE antibody (1:50). The anti-HDAC2 antibody was purchased from Abcam (Cambridge, UK), and the anti-4-HNE antibody was obtained from R&D Systems (USA). After several washes, the sections were treated with diaminobenzidine (DAB) and observed under a microscope.

2.4. Detection of TNF-α, IL-8 and 4-HNE concentration

The ELISA kit instructions (Jiangsu Enzyme Immune Industry Company) were strictly followed. The prepared samples were incubated and stained, and the optical density (OD) values were measured using microplate reader. Finally, the concentrations of 4-HNE and TNF-α were calculated using a linear equation derived from the standard curve.

2.5. Western blotting

Protein extraction from lung tissue was performed using RIPA lysis buffer and a protease inhibitor mixture, with protein concentration determined by a commercial kit. Protein samples were separated on 8 %–10 % SDS-PAGE and transferred to a polyvinylidene fluoride (PVDF) membrane. The membrane was blocked for 20 min on a shaker and incubated with primary antibodies: GAPDH (1:2000), MRP1 (1:50), and HDAC2 (1:2000) at 4 °C overnight. Anti-GAPDH was provided by Beijing Zhongshan Golden Bridge Company (Beijing, China), anti-MRP1 and anti-HDAC2 were supplied by Abcam (Cambridge, UK), and anti-GRα by Abways (Abways Technology). Afterward, the PVDF membrane was washed and incubated with corresponding secondary antibodies for 2 h at

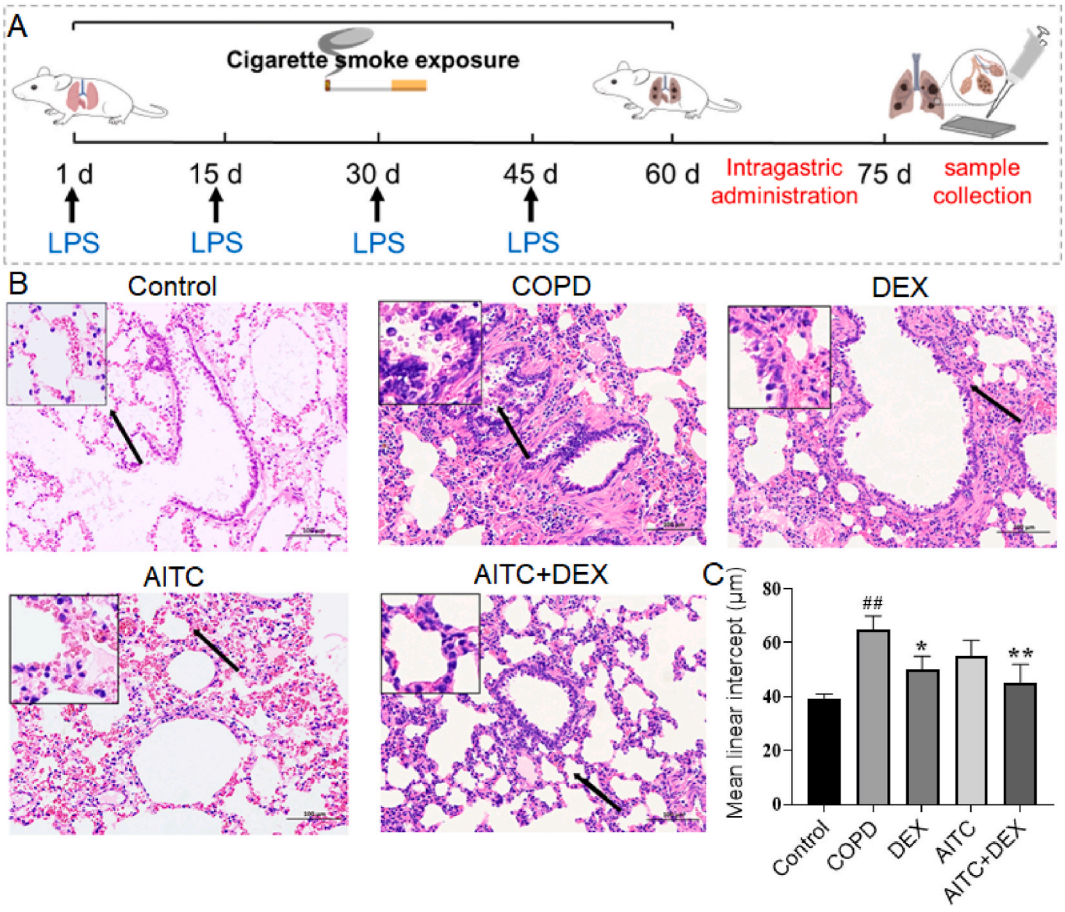

Fig. 1. AITC improves lung tissue injury in COPD rats. (A) Schematic diagram of animal experiment. (B) Results of pulmonary histopathology and (C) alveolar mean linear intercept. scale bar = 100 μm $^{\#\#}P < 0.01$ vs. Control group, $^{*}P < 0.05$ or $^{**}P < 0.01$ vs. COPD group.

room temperature. Finally, the membrane was uniformly covered with ECL luminescent solution (Biosharp, Hefei, China) and exposed to a chemiluminescence instrument. Protein gray values were analyzed using ImageJ software.

2.6. Cell culture and treatment

16HBE cells (RRID: CVCL 0112, Shanghai Sixin Biological Technology) were cultured in Dulbecco's Modified Eagle Medium (DMEM) supplemented with 10 % fetal bovine serum and 1 % penicillin/streptomycin, and then digested for passaging using trypsin after reaching 85 %–90 % confluence. Short tandem repeat (STR) analysis (2024.01) was used to verify the identity of 16HBE cells. MycoAlert mycoplasma detection kit (Lonza) was used to detect mycoplasma contamination in 16HBE cells. Then, 16HBE cells were exposed to various drug treatments for 2 h following 24 h of stimulation with 4-HNE. Subsequently, the cells were incubated with DEX at concentrations ranging from 10^{-10} to 10^{-6} mol/L for 1 h, followed by exposure to LPS (1 mg/L) for 24 h 16HBE cells were seeded into 96-well plates (1×10^4/well) and cultured for 24 h. Then, the cells were co-cultured with DEX, 4-HNE and AITC in a series of concentrations for 12 h, 24 h and 36 h. Finally, after treatment including co-incubation with CCK-8 (10 μL/well) for 1 h, the Uv–vis absorbance of cells in each well was measured at 450 nm with a microplate reader.

2.7. Determination of reactive oxygen species (ROS)

Intracellular ROS levels were measured using 2,7-dichlorofluorescein diacetate (DCFH-DA). Cells cultured in 6-well plates (2×10^5/well) were incubated with DCFH-DA (50 μmol/L) for 30 min. After incubation, the cells were washed three times with serum-free medium and then stimulated with low, medium, and high doses of 4-HNE for 30 min. Finally, the fluorescence intensity was measured using a fluorescence microscope (Leica, Wetzlar, Germany) at an excitation wavelength of 485 nm.

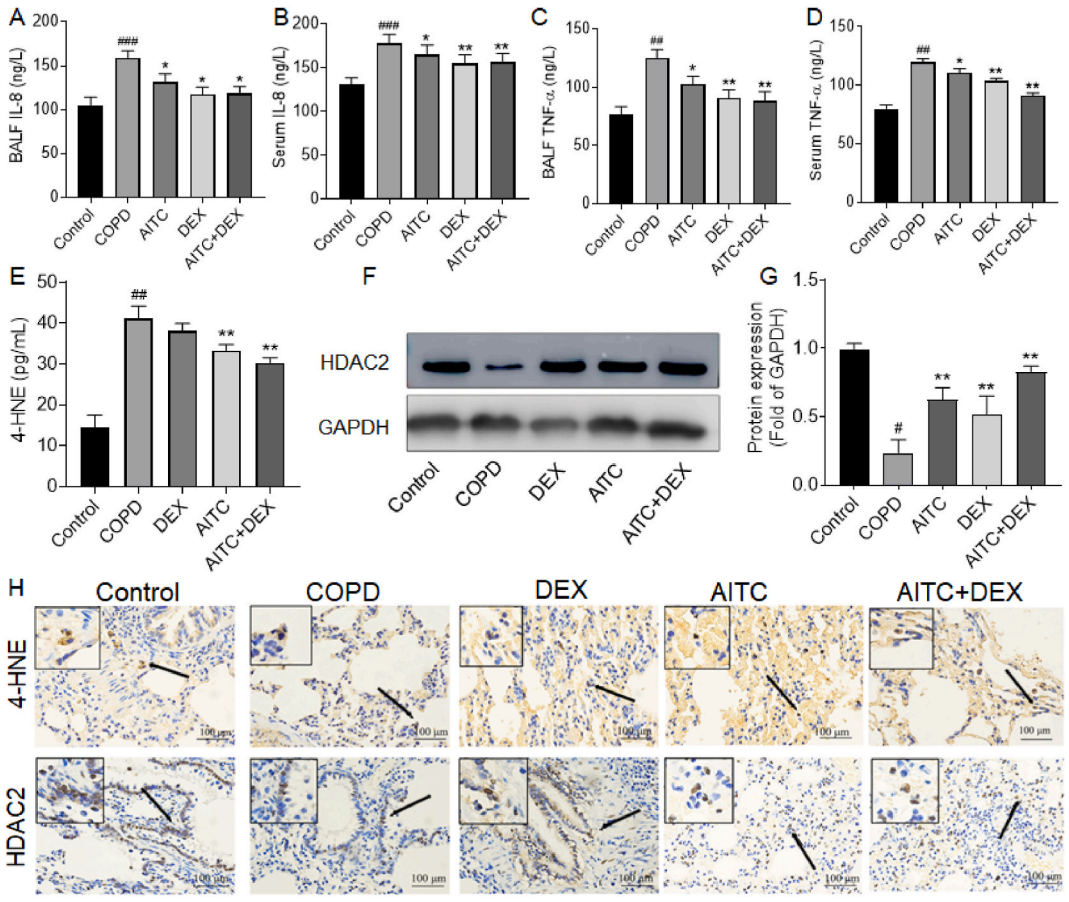

Fig. 2. AITC improves inflammatory response, lipid peroxidation and histone expression in COPD rats. Levels of inflammatory cytokines (A–B) IL-8 and (C–D) TNF-α in serum and BALF of rats, n = 6. $^{\#\#}P < 0.01$ vs. Control group, $^{*}P < 0.05$ or $^{**}P < 0.01$ vs. COPD group. (E) Expressions of 4-HNE in lung tissue of various group rats. (F) Western blot strip chart and (G) relative expression of HDAC2 protein in lung tissue of various group rats. (H) Immunohistochemical results of 4-HNE and HDAC2. Scale bar = 100 μm, $^{\#}P < 0.05$ Vs. Control group, $^{**}P < 0.01$ vs. COPD group, n = 6.

2.8. Statistical analysis

Statistical analyses were performed using GraphPad Prism 8.0 (GraphPad Prism, United States). The experimental data were expressed as mean ± standard deviation (SD). One-way analysis of variance followed by Tukey's multiple comparison test was used to analysis differences between groups. Statistical significance was defined as a *P* value less than 0.05.

3. Result

3.1. Effects of AITC on lung inflammation, function and damage in COPD rats

To ascertain whether the COPD could respond to oxidative stress, SD rats were exposed to CSE and LPS and their inflammation and lipid peroxidation were measured. As shown in Table S1, lung function indices such as FEV0.3/FVC %, FEF25-75, MMF, and PEF were significantly reduced in the model group compared to the control group ($P < 0.01$). However, The AITC group had the opposite effect. This was especially true in the AITC + DEX group. Additionally, as shown in Fig. 1B and C, H&E staining analysis of lung tissues demonstrated that long-term smoking caused significant infiltration of inflammatory cells around the bronchi and alveoli, and rupture of the alveolar structure. The pathological damage of lung tissue in the AITC group was significantly improved compared with the model group, especially the effect of AITC + DEX was more obvious. Furthermore, as shown in Table S2, in the COPD model group,

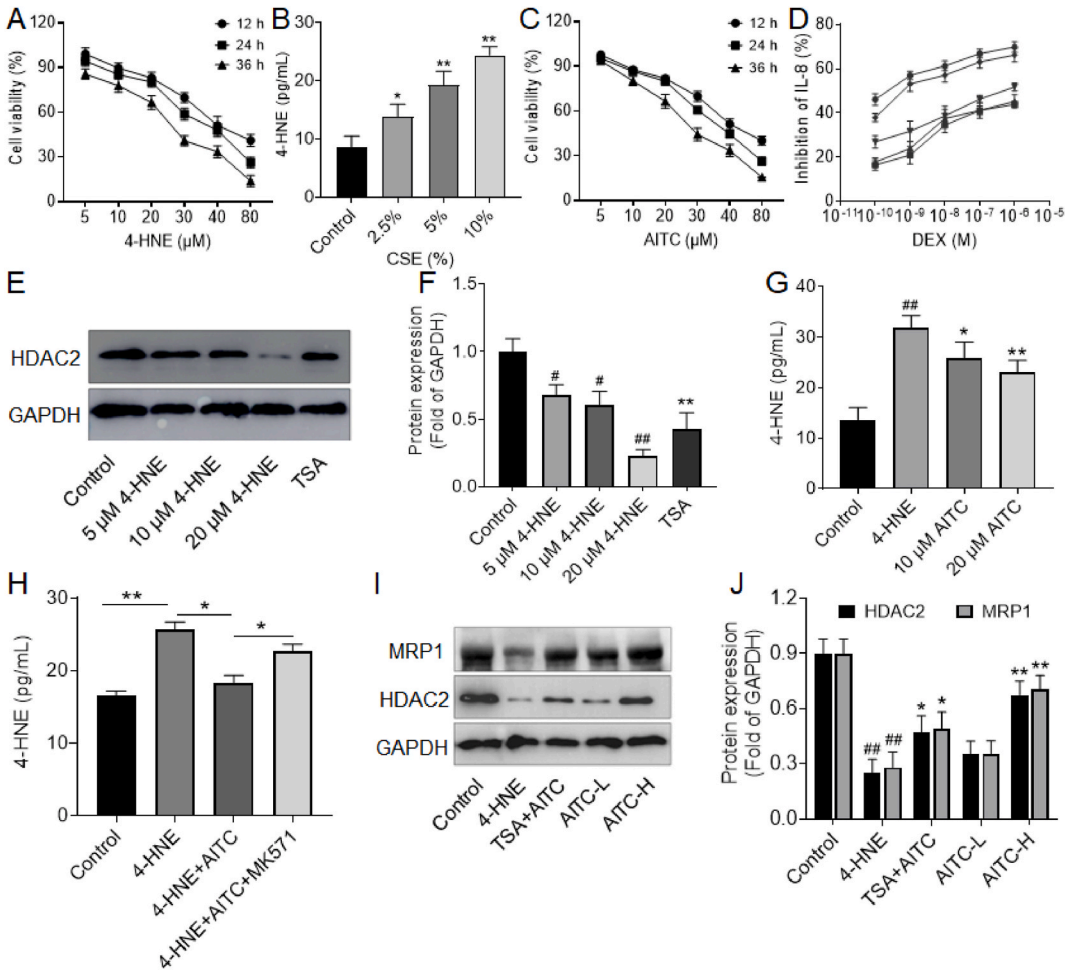

Fig. 3. MRP1 and HDAC2 protein expression and 4-HNE levels in rats. (A) Effects of 4-HNE on cell viability of 16HBE cells. (B) Effect of different concentrations of CSE on 4-HNE levels. $^{*}P < 0.05$ or $^{**}P < 0.01$ vs. Control group, n = 3. (C) Survival of 16HBE in the presence of different concentrations of AITC for 12, 24, and 36 h. (D) Effect of AITC on IL-8 inhibition rates in each group. (E) Western blot strip chart and (F) relative expression of HDAC2 protein in 16HBE cells through 4-HNE intervention. $^{\#}P < 0.05$ vs. Control group, $^{**}P < 0.01$ vs. 5 μM 4-HNE group, n = 3. (G) Effect of AITC on the level of 4-HNE in 16HBE cells. $^{\#\#}P < 0.01$ vs. Control group, $^{*}P < 0.05$ or $^{**}P < 0.01$ vs. 4-HNE group, n = 3. (H) The effect of AITC on the level of 4-HNE in 16HBE cells under the intervention of MRP1. $^{\#\#}P < 0.01$ vs. Control group, $^{*}P < 0.05$ vs. 4-HNE group or 4-HNE + AITC, n = 3. (I) Western blot strip chart and (J) relative expression of HDAC2 and MRP1 protein expression in GC-resistant cells. AITC-L: AITC low-dose group; AITC-H: AITC high-dose group. $^{\#\#}P < 0.01$ vs. Control group, $^{*}P < 0.05$ or $^{**}P < 0.01$ vs. 4-HNE group, n = 3.

macrophages were significantly reduced, while the proportion of neutrophils, eosinophils, and total white blood cells significantly increased. The AITC + DEX group and the AITC group showed an opposite trend ($P < 0.05$). Moreover, as shown in Fig. 2A–D, the concentrations of IL-8 and TNF-α in the COPD model group were significantly higher than those in the control group ($P < 0.01$). BALF and serum levels of inflammatory factors were significantly reduced in the group co-treated with DEX and AITC ($P < 0.05$). These results suggest that AITC has a reversing effect on lung inflammation in rats with COPD.

3.2. AITC reduces the level of 4 - HNE and up-regulates the expression of HDAC2

COPD not only induces inflammation and tissue damage but also increases lipid peroxidation, which is associated with oxidative stress. To determine whether COPD could induce oxidative stress, SD rats were exposed to cigarette smoke (CS), and lipid peroxidation was measured. As shown in Fig. 2E, the content of 4-HNE was significantly increased in the model group ($P < 0.01$). AITC and DEX reduced the serum content of 4-HNE in the COPD groups ($P < 0.05$). Importantly, as shown in Fig. 2F and G, HDAC2 protein expression was inhibited in COPD rats compared to the control group; however, AITC significantly increased HDAC2 expression ($P < 0.01$). To investigate whether AITC regulates HDAC2 expression through modulation of 4-HNE levels, immunohistochemistry was employed to analyze the expression of 4-HNE and HDAC2 proteins. As shown in Fig. 2H, HDAC2 expression was lower in the model group compared to the control group. However, it was upregulated following AITC and DEX treatment, and 4-HNE expression was downregulated, suggests that AITC may increase HDAC2 expression in the lungs of COPD rats by reducing 4-HNE levels. These results indicated that the smoking-induced COPD not only increases lipid peroxidation associated with oxidative stress but also impedes GC-induced histone deacetylation. The high expression of 4-HNE in COPD rats may be closely related to the expression of HDAC2 protein, and AITC could up-regulate the expression of HDAC2. Suggested that AITC has therapeutic potential in restoring glucocorticoid sensitivity in COPD patients, thereby improving treatment outcomes.

3.3. AITC increased the sensitivity of 16HBE cells to DEX

To evaluate the effect of the oxidative stress product 4-HNE on GC resistance in COPD, we used the CCK8 assay to determine cell viability. As shown in Fig. 3A, cell viability remained above 80 % after 24 h stimulation with 5 μM 4-HNE. Therefore, 5 μM 4-HNE was used to stimulate 16HBE cells for 24 h in the glucocorticoid resistance experiment. Subsequently, as shown in Fig. 3B, the level of 4-HNE in 16HBE cells was significantly increased after 2.5 %, 5 % and 10 % CSE intervention for 24 h, indicating that CSE stimulation increased the level of 4-HNE in 16HBE cells.

As shown in Fig. 3C, the cytotoxic effects of AITC on 16HBE cells were assessed using the CCK-8 assay. The results indicated that AITC inhibited cell viability in a concentration-dependent manner, with 5 μM, 10 μM, and 20 μM chosen as low, medium, and high intervention concentrations, respectively, and incubated with 16HBE cells for 24 h. Finally, the inhibitory effects of various concentrations of DEX (10^{-10} to 10^{-6} mol/L) on IL-8 release were determined, and the $IC_{50\text{-DEX}}$ was used to assess GC sensitivity. To investigate whether AITC enhances the sensitivity of 16HBE cells to DEX induced by 4-HNE through HDAC2 modulation, its inhibitor trichostatin A (TSA) was co-administered with AITC. As shown in Fig. 3D and Table S3, the $IC_{50\text{-DEX}}$ in the 4-HNE group was significantly increased ($P < 0.01$). The $IC_{50\text{-DEX}}$ value in the AITC-H treatment group was significantly lower than that in the 4-HNE group (P

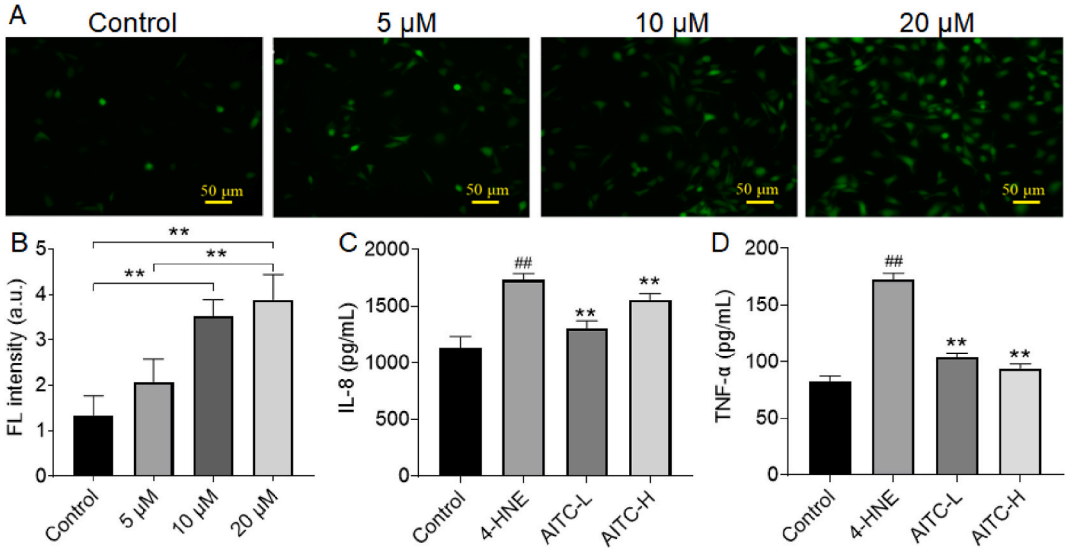

Fig. 4. AITC improves intracellular oxidative stress and inflammation. (A) 4-HNE induced intracellular ROS. (B) Fluorescence intensity represents intracellular ROS levels, $^{\#}P < 0.05$ or $^{\#\#}P < 0.01$vs. Control group, $^{*}P < 0.05$ or $^{**}P < 0.01$ vs. 5 μM group, n = 3. Levels of inflammatory cytokines (C) IL-8 and (D) TNF-α in 16HBE cells. $^{\#\#}P < 0.01$ vs. Control group, $^{**}P < 0.01$vs. 4-HNE group, n = 3.

< 0.05). However, the decrease of $IC_{50\text{-}DEX}$ was inhibited by the combination of AITC-H and TSA. The above results suggest that AITC may increase the sensitivity of 16HBE cells to glucocorticoids under 4-HNE stimulation by regulating the expression of HDAC2.

3.4. Effect of AITC on HDAC2, 4-HNE, and MRP1

To investigate the impact of 4-HNE on HDAC2 expression in 16HBE cells, cells were exposed to 5 μM, 10 μM, and 20 μM concentrations of 4-HNE for 24 h. As illustrated in Fig. 3E and F, 4-HNE reduced HDAC2 expression in a concentration-dependent manner ($P < 0.01$). Subsequently, 16HBE cells were pre-incubated with different concentrations of AITC for 2 h, and then stimulated with 5 μM 4-HNE for 24 h. As shown in Fig. 3G, AITC treatment significantly reduced 4-HNE levels compared to the 4-HNE group ($P < 0.05$). Importantly, since 4-HNE is an affinity substrate for MRP1, it is crucial to understand the role of MRP1 in the reduction of glucocorticoid resistance by AITC. Subsequently, as depicted in Fig. 3H, the MRP1 inhibitor MK571 was used to inhibit MRP1 activity. The 4-HNE levels in the MK571 + AITC group were significantly higher than those in the AITC group ($P < 0.01$). This indicated that the ability of AITC to inhibit 4-HNE was weakened when the expression of MRP1 was inhibited.

Next, the protein expression levels of MRP1 and HDAC2 were assessed by Western blotting to elucidate the mechanism by which AITC reduces glucocorticoid resistance. As shown in Fig. 3I and J, the expression levels of MRP1 and HDAC2 proteins were significantly decreased in the 4-HNE group compared to the control group. Furthermore, compared to the 4-HNE group, the expression levels of MRP1 and HDAC2 proteins were restored in the AITC-H group and the AITC + TSA combined treatment group ($P < 0.05$), with particularly notable effects in the AITC-H group. These results suggest that AITC can upregulate the expression of HDAC2 and MRP1 in a dose-dependent manner. Thus, the effect of AITC on enhancing GC resistance may involve upregulating MRP1 protein expression by reducing 4-HNE levels, which in turn regulates HDAC2 protein expression.

3.5. Effects of 4-HNE on ROS and TNF-α in 16HBE cells

To evaluate the effect of the peroxidation product 4-HNE on oxidative stress in COPD, changes in the intensity of ROS fluorescence and in the levels of inflammatory factors in 16HBE cells were detected. As shown in Fig. 4A and B, ROS levels and fluorescence intensity were significantly elevated in the 10 μM and 20 μM 4-HNE treatment groups compared to the control group ($P < 0.05$). Additionally, as demonstrated in Fig. 4C and D, the concentrations of IL-8 and TNF-α were significantly higher in the 4-HNE group ($P < 0.01$). Treatment with AITC significantly reduced the concentrations of IL-8 and TNF-α ($P < 0.01$), exogenous stimulation with 4-HNE of 16HBE cells exhibits substantial a dose-dependent toxicity, increased the levels of TNF-α and ROS, indicating that smoking could enhance oxidative stress and damage cells.

4. Discussion

Chronic obstructive pulmonary disease (COPD) is a prevalent chronic lung condition characterized by inflammation, airway obstruction, and lung damage. It has long been associated with smoking [21]. Upon entering the respiratory tract, cigarette smoke activates airway epithelial cells and macrophages to release various chemokines, which recruit neutrophils and lymphocytes. Studies have shown that the number of neutrophils in the sputum of COPD patients is increased, along with the secretion of neutrophil elastase and matrix metalloproteinases (MMPs), leading to alveolar structure damage [22]. Additionally, the abundant oxidants and electrophiles in cigarette smoke can induce oxidative stress by generating numerous free radicals in vivo, which attack unsaturated fatty acids in bronchial epithelial cells and produce active lipid peroxides. The active aldehyde 4-HNE is a lipid peroxidation product, and its intracellular accumulation at concentrations ranging from 10 μM to 5 mM leads to severe oxidative damage compared to physiological serum levels. Furthermore, 4-HNE effectively induces ROS, which is accompanied by the accumulation of ubiquitinated proteins and apoptosis [23,24]. The antioxidant defense mechanisms of the lungs protect against the harmful effects of oxidants through electron transfer, enzymatic removal, clearance, and maintenance of tight isolation of transition metal ions [25]. Moreover, the detoxification of reactive aldehydes in cellular oxidative metabolism is mediated by aldehyde dehydrogenases and aldehyde ketone reductase, which decarbonylate proteins to reverse the post-translational modifications they induce [26]. However, cigarette smoke increases reactive oxygen species and decreases endogenous antioxidant defenses, affecting the activity of dehydrogenases and reductases, and leading to the accumulation of significant amounts of reactive aldehydes intracellularly [27].

The HDAC family can remove the acetyl group from histones, inducing DNA condensation to silence gene transcription. Additionally, it has the capability to deacetylate non-histone proteins, modulating NF-κB-dependent pro-inflammatory gene transcription [28]. Importantly, HDAC2 expression and activity are significantly reduced in COPD due to post-translational modifications such as nitrosylation, phosphorylation, and ubiquitination. This leads to protease-dependent degradation, particularly in response to the severity of COPD and the intensity of inflammation [29]. Therefore, GCs induce the decarboxylation or dephosphorylation of HDAC2 by aldehyde dehydrogenases/reductases or phosphatases, reversing the post-translational modifications of HDAC2 and enhancing sensitivity to the GC receptor [30].

In this work, we observed significant levels of the lipid peroxidation product 4-HNE in the lung tissues and bronchial epithelial cells of COPD rats induced by cigarette smoke and LPS. Furthermore, HDAC2 protein expression exhibited a significant decrease in CSE-induced COPD 16HBE cells following exogenous stimulation with 4-HNE, leading to a substantial reduction in the efficacy of DEX intervention. This confirms that GC resistance observed in COPD is attributed to the accumulation of lipid peroxidation-related products caused by the disruption of the intracellular redox balance by reactive oxygen species. These substances significantly decrease the expression and activity of HDAC2, impeding the deacetylation process of histones and preventing the completion of the

anti-inflammatory effects of GCs. Therefore, an effective strategy to remove peroxidation products would indirectly reduce GC resistance in COPD treatment.

Naturally occurring phytochemicals, such as baicalin, quercetin, resveratrol, Epigallocatechin gallate (EGCG), and curcumin, are gaining popularity for COPD treatment due to their safety, bioavailability, efficacy, and easy accessibility [31,32]. Allyl isothiocyanate (AITC, $CH_2{=}CHCH_2N{=}C{=}S$ or C_4H_5NS) is a natural compound found in all cruciferous vegetables. It is produced by the hydrolysis of the glucosinolate sinigrin by the enzyme myrosinase, with nearly 90 % of orally supplemented AITC being absorbed, indicating exceedingly high bioavailability. Furthermore, AITC regulates oxidative stress, inflammation, cell proliferation, cell cycle arrest, apoptosis, angiogenesis, invasion, and metastasis through interactions with multiple cells signaling pathways [33]. Additionally, AITC has anti-inflammatory activity, which is beneficial to improve chronic respiratory disease [19]. AITC exhibits potent anti-inflammatory and antiasthmatic effects by inhibiting airway inflammation, tracheal constriction, and airway remodeling, while also increasing the expression of tight-junction proteins through the TRPA1 channel [34].

MRP1 belongs to the ATP-binding cassette (ABC) transporter family [30]. Its overexpression or abnormal activation demonstrates a wide range of physiological functions, such as the cellular efflux of drugs and transport of metabolites, which are closely associated with multidrug resistance and detoxification [35]. Moreover, MRP1 expression is regulated by various factors, including genetic, post-transcriptional, and protein stability mechanisms, as well as certain drugs and compounds. We have confirmed that AITC can up-regulate the activity of MRP1 via the Notch1/Hes1 and DJ-1/Nrf2 pathways, demonstrating remarkable efficacy in COPD-related studies [19]. In this study, MRP1 serves as a transporter for the efflux of cellular oxidative stress metabolites. Its enhanced activity under AITC regulation could significantly transport 4-HNE to the extracellular space, ultimately upregulating HDAC2 protein expression in tissues and cells. Notably, the short duration of treatment and the absence of clinical evaluation are areas that need to be addressed in future developments. These results have great potential for restoring lung function, reducing inflammatory cells and associated factors, and attenuating lung tissue damage in GC-resistant COPD.

5. Conclusion

This work highlighted the development of GC resistance in COPD, induced by abundant oxygen free radicals from cigarette smoke. It endows the cells with oxidative stress damage and disorder of lipid peroxidation metabolism, leading to the intracellular accumulation of the toxic product 4-HNE, thereby hindering HDAC2-mediated histone deacetylation, and reducing sensitivity to GCs. AITC could restore GC sensitivity, achieve the restoration of lung function and alleviation of inflammation in COPD rats, owing to its significant enhancement of MRP1 activity to effectively extrude 4-HNE and reduce HDAC2 damage. Therefore, such AITC-regulated oxidative stress holds great potential for targeted therapy of GC resistance in COPD, but still focusing on the long-term efficacy and safety of AITC in COPD models and conducting clinical trials to validate these findings in patients.

Data availability

Data will be made available on request.

CRediT authorship contribution statement

WenLi Chang: Writing – original draft, Methodology, Investigation, Conceptualization. **MengWen Wang:** Methodology, Data curation. **WenTao Zhu:** Resources, Formal analysis. **TingTing Dai:** Validation. **ZhiLi Han:** Writing – review & editing. **NianXia Sun:** Writing – review & editing. **DianLei Wang:** Writing – review & editing.

Declaration of competing interest

The authors declare that they have no known competing financial interests or personal relationships that could have appeared to influence the work reported in this paper.

Acknowledgements

The work was financially supported by Natural Science Foundation of Anhui Provincial (No: 2108085J45) and Natural Science Research Project of Anhui Educational Committee (No: 2022AH050498).

Appendix A. Supplementary data

Supplementary data to this article can be found online at https://doi.org/10.1016/j.heliyon.2024.e37275.

References

[1] P. Upadhyay, C.W. Wu, A. Pham, A.A. Zeki, C.M. Royer, U.P. Kodavanti, M. Takeuchi, H. Bayram, K.E. Pinkerton, Animal models and mechanisms of tobacco smoke-induced chronic obstructive pulmonary disease (COPD), J. Toxicol. Environ. Health B Crit. Rev. 26 (2023) 275–305, https://doi.org/10.1080/10937404.2023.2208886.

[2] S.P. Lakshmi, A.T. Reddy, R.C. Reddy, Emerging pharmaceutical therapies for COPD, Int. J. Chronic Obstr. Pulm. Dis. 12 (2017) 2141–2156, https://doi.org/10.2147/COPD.S121416.

[3] P.J. Barnes, R.A. Stockley, COPD: current therapeutic interventions and future approaches, Eur. Respir. J. 25 (2005) 1084–1106, https://doi.org/10.1183/09031936.05.00139104.

[4] R.N. Criner, M.K. Han, COPD care in the 21st century: a public health priority, Respir. Care 63 (2018) 591–600, https://doi.org/10.4187/respcare.06276.

[5] P.J. Barnes, Glucocorticosteroids, Handb. Exp. Pharmacol. 237 (2017) 93–115, https://doi.org/10.1007/164_2016_62.

[6] P.J. Barnes, I.M. Adcock, Glucocorticoid resistance in inflammatory diseases, Lancet 373 (2009) 1905–1917, https://doi.org/10.1016/S0140-6736(09)60326-3.

[7] A.T. Reddy, S.P. Lakshmi, A. Banno, R.C. Reddy, Glucocorticoid receptor alpha mediates roflumilast's ability to restore dexamethasone sensitivity in COPD, Int. J. Chronic Obstr. Pulm. Dis. 15 (2020) 125–134, https://doi.org/10.2147/COPD.S230188.

[8] T. van den Bosch, N.G.J. Leus, H. Wapenaar, A. Boichenko, J. Hermans, R. Bischoff, H.J. Haisma, F.J. Dekker, A 6-alkylsalicylate histone acetyltransferase inhibitor inhibits histone acetylation and pro-inflammatory gene expression in murine precision-cut lung slices, Pulm. Pharmacol. Ther. 44 (2017) 88–95, https://doi.org/10.1016/j.pupt.2017.03.006.

[9] A. Tamimi, D. Serdarevic, N.A. Hanania, The effects of cigarette smoke on airway inflammation in asthma and COPD: therapeutic implications, Respir. Med. 106 (2012) 319–328, https://doi.org/10.1016/j.rmed.2011.11.003.

[10] D. Malhotra, R.K. Thimmulappa, N. Mercado, K. Ito, P. Kombairaju, S. Kumar, J. Ma, D. Feller-Kopman, R. Wise, P. Barnes, S. Biswal, Denitrosylation of HDAC2 by targeting Nrf2 restores glucocorticosteroid sensitivity in macrophages from COPD patients, J. Clin. Invest. 121 (2011) 4289–4302, https://doi.org/10.1172/JCI45144.

[11] D. Adenuga, H. Yao, T.H. March, J. Seagrave, I. Rahman, Histone deacetylase 2 is phosphorylated, ubiquitinated, and degraded by cigarette smoke, Am. J. Respir. Cell Mol. Biol. 40 (2009) 464–473, https://doi.org/10.1165/rcmb.2008-0255OC.

[12] M.J. Randall, G.R. Haenen, F.G. Bouwman, A. van der Vliet, A. Bast, The tobacco smoke component acrolein induces glucocorticoid resistant gene expression via inhibition of histone deacetylase, Toxicol. Lett. 240 (2016) 43–49, https://doi.org/10.1016/j.toxlet.2015.10.009.

[13] H. Kume, R. Yamada, Y. Sato, R. Togawa, Airway smooth muscle regulated by oxidative stress in COPD, Antioxidants 12 (2023), https://doi.org/10.3390/antiox12010142.

[14] D. Nowak, M. Janczak, Effect of chemotherapy on serum end-products of lipid peroxidation in patients with small cell lung cancer: association with treatment results, Respir. Med. 100 (2006) 157–166, https://doi.org/10.1016/j.rmed.2005.04.002.

[15] H. Yao, I. Edirisinghe, S.R. Yang, S. Rajendrasozhan, A. Kode, S. Caito, D. Adenuga, I. Rahman, Genetic ablation of NADPH oxidase enhances susceptibility to cigarette smoke-induced lung inflammation and emphysema in mice, Am. J. Pathol. 172 (2008) 1222–1237, https://doi.org/10.2353/ajpath.2008.070765.

[16] M. van der Deen, E.G. de Vries, H. Visserman, W. Zandbergen, D.S. Postma, W. Timens, H. Timmer-Bosscha, Cigarette smoke extract affects functional activity of MRP1 in bronchial epithelial cells, J. Biochem. Mol. Toxicol. 21 (2007) 243–251, https://doi.org/10.1002/jbt.20187.

[17] M.A. Selo, A.S. Delmas, L. Springer, V. Zoufal, J.A. Sake, C.G. Clerkin, H. Huwer, N. Schneider-Daum, C.M. Lehr, S. Nickel, O. Langer, C. Ehrhardt, Tobacco smoke and inhaled drugs alter expression and activity of multidrug resistance-associated protein-1 (MRP1) in human distal lung epithelial cells in vitro, Front. Bioeng. Biotechnol. 8 (2020) 1030, https://doi.org/10.3389/fbioe.2020.01030.

[18] W.T. Zhu, C.H. Li, T.T. Dai, Q.Q. Song, Y. Chen, Z.L. Han, N.X. Sun, D.L. Wang, Effect of allyl isothiocyanate on oxidative stress in COPD via the AhR/CYP1A1 and Nrf2/NQO1 pathways and the underlying mechanism, Phytomedicine 114 (2023) 154774, https://doi.org/10.1016/j.phymed.2023.154774.

[19] Y. Zhou, X. Xu, J. Wu, L. Xu, M. Zhang, Z. Li, D. Wang, Allyl isothiocyanate treatment alleviates chronic obstructive pulmonary disease through the Nrf2-Notch1 signaling and upregulation of MRP1, Life Sci. 243 (2020) 117291, https://doi.org/10.1016/j.lfs.2020.117291.

[20] W.T. Zhu, C.H. Li, T.T. Dai, F.L. Tao, M.W. Wang, C.Y. Wang, Z.L. Han, N.X. Sun, Y.N. Zhao, D.L. Wang, Effects of allyl isothiocyanate on the expression, function, and its mechanism of ABCA1 and ABCG1 in pulmonary of COPD rats, Int. Immunopharm. 101 (2021) 108373, https://doi.org/10.1016/j.intimp.2021.108373.

[21] K.U. Alwis, B.R. deCastro, J.C. Morrow, B.C. Blount, Acrolein exposure in U.S. Tobacco smokers and non-tobacco users: NHANES 2005-2006, Environ. Health Perspect. 123 (2015) 1302–1308, https://doi.org/10.1289/ehp.1409251.

[22] Y. Wang, M. Jia, X. Yan, L. Cao, P.J. Barnes, I.M. Adcock, M. Huang, X. Yao, Increased neutrophil gelatinase-associated lipocalin (NGAL) promotes airway remodelling in chronic obstructive pulmonary disease, Clin. Sci. 131 (2017) 1147–1159, https://doi.org/10.1042/CS20170096.

[23] A.J. McGuinness, E. Sapey, Oxidative stress in COPD: sources, markers, and potential mechanisms, J. Clin. Med. 6 (2017), https://doi.org/10.3390/jcm6020021.

[24] G.D. Albano, R.P. Gagliardo, A.M. Montalbano, M. Profita, Overview of the mechanisms of oxidative stress: impact in inflammation of the airway diseases, Antioxidants 11 (2022), https://doi.org/10.3390/antiox11112237.

[25] Y. Kabuyama, T. Suzuki, N. Nakazawa, J. Yamaki, M.K. Homma, Y. Homma, Dysregulation of very long chain acyl-CoA dehydrogenase coupled with lipid peroxidation, Am. J. Physiol. Cell Physiol. 298 (2010) C107–C113, https://doi.org/10.1152/ajpcell.00231.2009.

[26] Y. Yamauchi, A. Hasegawa, A. Taninaka, M. Mizutani, Y. Sugimoto, NADPH-dependent reductases involved in the detoxification of reactive carbonyls in plants, J. Biol. Chem. 286 (2011) 6999–7009, https://doi.org/10.1074/jbc.M110.202226.

[27] M.H. Liu, A.H. Lin, H.F. Lee, H.K. Ko, T.S. Lee, Y.R. Kou, Paeonol attenuates cigarette smoke-induced lung inflammation by inhibiting ROS-sensitive inflammatory signaling, Mediat. Inflamm. 2014 (2014) 651890, https://doi.org/10.1155/2014/651890.

[28] S. Bahl, H. Ling, N.P.N. Acharige, I. Santos-Barriopedro, M.K.H. Pflum, E. Seto, EGFR phosphorylates HDAC1 to regulate its expression and anti-apoptotic function, Cell Death Dis. 12 (2021) 469, https://doi.org/10.1038/s41419-021-03697-6.

[29] L. Li, H. Bao, J. Wu, X. Duan, B. Liu, J. Sun, W. Gong, Y. Lv, H. Zhang, Q. Luo, X. Wu, J. Dong, Baicalin is anti-inflammatory in cigarette smoke-induced inflammatory models in vivo and in vitro: a possible role for HDAC2 activity, Int. Immunopharm. 13 (2012) 15–22, https://doi.org/10.1016/j.intimp.2012.03.001.

[30] J. Bi, Z. Min, H. Yuan, Z. Jiang, R. Mao, T. Zhu, C. Liu, Y. Zeng, J. Song, C. Du, Z. Chen, PI3K inhibitor treatment ameliorates the glucocorticoid insensitivity of PBMCs in severe asthma, Clin. Transl. Med. 9 (2020) 22, https://doi.org/10.1186/s40169-020-0262-5.

[31] S.P. Lakshmi, A.T. Reddy, L.D. Kodidhela, N.C. Varadacharyulu, Epigallocatechin gallate diminishes cigarette smoke-induced oxidative stress, lipid peroxidation, and inflammation in human bronchial epithelial cells, Life Sci. 259 (2020) 118260, https://doi.org/10.1016/j.lfs.2020.118260.

[32] L.Y. Li, C.T. Zhang, F.Y. Zhu, G. Zheng, Y.F. Liu, K. Liu, C.H. Zhang, H. Zhang, Potential natural small molecular compounds for the treatment of chronic obstructive pulmonary disease: an overview, Front. Pharmacol. 13 (2022) 821941, https://doi.org/10.3389/fphar.2022.821941.

[33] T. Rajakumar, P. Pugalendhi, Allyl isothiocyanate regulates oxidative stress, inflammation, cell proliferation, cell cycle arrest, apoptosis, angiogenesis, invasion and metastasis via interaction with multiple cell signaling pathways, Histochem, Cell Biol. 161 (2024) 211–221, https://doi.org/10.1007/s00418-023-02255-9.

[34] Y.H. Lai, Y.F. Chiang, K.C. Huang, H.Y. Chen, M. Ali, S.M. Hsia, Allyl isothiocyanate mitigates airway inflammation and constriction in a house dust mite-induced allergic asthma model via upregulation of tight junction proteins and the TRPA1 modulation, Biomed. Pharmacother. 166 (2023) 115334, https://doi.org/10.1016/j.biopha.2023.115334.

[35] L.P. Rudd, S.L. Kabler, C.S. Morrow, A.J. Townsend, Enhanced glutathione depletion, protein adduct formation, and cytotoxicity following exposure to 4-hydroxy-2-nonenal (HNE) in cells expressing human multidrug resistance protein-1 (MRP1) together with human glutathione S-transferase-M1 (GSTM1), Chem. Biol. Interact. 194 (2011) 113–119, https://doi.org/10.1016/j.cbi.2011.08.012.